Monitoring statistics of the
ERS-2 scatterometer for ESA

Cycle 158

Hans Hersbach

European Centre for Medium-Range Weather Forecasts,
Shinfield Park, Reading, RG2 9AX, England
Tel: (+44 118) 9499476, e-mail: dal@ecmwf.int

July 6, 2010

1   Introduction

The quality of the UWI product was monitored at ECMWF for Cycle 158. Results were compared to those obtained from the previous Cycle, as well for data received during the nominal period in 2000 (up to Cycle 59). No corrections for duplicate observations from overlapping ground stations were applied.

During Cycle 158 data was received between 21:04 UTC 31 May 2010 and 20:59 UTC 5 July 2010. Data was grouped into 6-hourly batches (centred around 00, 06, 12 and 18 UTC). No data was received for the batches cantered around 18 UTC 9 June 2010, 12 UTC 15 June 2010, 18 UTC 22 June 2010, 12 UTC 23 June 2010, 18 UTC 1 July 2010, 18 UTC 3 July 2010, and 18 UTC 5 July 2010.

Data is being recorded whenever within the visibility range of a ground station. For Cycle 158, data coverage was over the North-Atlantic, the Mediterranean, the Gulf of Mexico, a very small part of the Pacific west from the US, Canada and Central America, the Chinese Sea, and a sparse area near Antarctica and south from Australia (see Figure 2).

Time series of the asymmetry between the fore and aft incidence angles show a reasonably calm behaviour, although there was an increased volatility near the end of Cycle 158.

Compared to Cycle 157, the UWI wind speed relative to ECMWF first-guess (FG) fields showed a reduced standard deviation (1.33 m/s, was 1.38 m/s). Bias levels were more negative (on average -1.08 m/s, was -1.03 m/s).

Ocean calibration shows that inter-node and inter-beam dependencies of bias levels have increased. Average bias levels were more negative (-0.98 dB, was -0.80 dB; see

Figure 4).

Time series for data volume, relative bias in wind speed, standard deviation in wind direction and for attitude control all indicate an increased volatility in the UWI product near the end of Cycle 158. At this moment, the lack in statistical significance does not allow for further statements on the stability of the UWI data.

The ECMWF operational assimilation and forecast system was changed on 22 June 2010, which mainly involved the ensemble prediction system. No significant effect on the quality of ECMWF surface wind is anticipated.

The Cycle-averaged evolution of performance relative to ECMWF first-guess (FG) winds is displayed in Figure 1. Figure 2 shows global maps of the over Cycle 158 averaged UWI data coverage and wind climate, Figure 3 for performance relative to FG winds.

2   ERS-2 statistics from 31 May 2010 to 5 July 2010

2.1   Sigma0 bias levels

The average sigma0 bias levels (compared to simulated sigma0's based on ECMWF model FG winds) stratified with respect to antenna beam, ascending or descending track and as function of incidence angle (i.e. across-node number) is displayed in Figure 4.

Compared to Cycle 157, inter-node and inter-beam dependencies between the fore and aft have further increased. Average bias level was more negative (-0.98 dB, was -0.80 dB), being 0.6 dB more negative than for nominal data in 2000 (around -0.4 dB; see Figure 1 of the reports for Cycle 48 to 59). The situation is similar to that of one year ago (see report for Cycle 148).

Long-term variations correlate with the yearly cycle, which, given the non-global coverage, is understandable. Therefore, the method of ocean calibration will probably only provide accurate information on calibration levels for globally or yearly averaged data sets.

The data volume of descending tracks was about 51% lower than for ascending tracks.

2.2   Incidence angles

For ESACA, across-node binning is, like the old processor, retained on a 25km mesh. From simple geometrical arguments it follows that variations in yaw attitude will lead to asymmetries between the incidence angles of the fore and aft beam. Indeed, this has been observed. Figure 5 gives a time evolution of this asymmetry. Also in this Figure, the occasions for which the combined k_p-yaw quality flag was set are indicated by red stars. The relation with incidence-angle asymmetries is obvious.

The asymmetry between the fore and aft incidence angles showed some rather large peaks, and especially near the end of Cycle 158 an increased volatility is observed.

After a prolonged minimum, solar activity is on the rise. Around 16 July 2010, solar wind caused a geomagnetic storm (source: www.spaceweather.com). These events did not seem to have an effect on ERS-2 attitude control.

2.3 Distance to cone history

The distance to the cone history is shown in Figure 6. Curves are based on data that passed all QC, including the test on the k_p-yaw flag, and subject to the land and sea-ice check at ECMWF (see cyclic report 88 for details).

Like for previous Cycles, time series are (due to lack of statistics) very noisy, especially for the near-range nodes. Most spikes were found to be the result of low data volumes.

Compared to Cycle 157, the average level increased (1.33, was 1.27), and is higher (by 22%) than for nominal data (see top panel Figure 1).

The fraction of data that did not pass QC is displayed in Figure 6 as well (dashed curves).

2.4 UWI minus First-Guess wind history

In Figure 7, the UWI minus ECMWF first-guess wind-speed history is plotted. The history plot shows a few peaks, which are usually the result of low data volume. An decrease in the negative relative bias seems to emerge from the last few days of Cycle 158.

Figure 11 displays the locations for which UWI winds were more than 8 m/s weaker (top panel), respectively more than 8 m/s stronger (lower panel) than FG winds. Like for Cycle 157, such collocations are isolated, and often indicate meteorologicaly active regions, for which UWI data and ECMWF model field show reasonably small differences in phase and/or intensity. Deviations near the poles are the result of imperfect sea-ice flagging.

Two cases for which UWI winds were considerably different from FG winds are presented in Figure 12. Both are near the coast of West Africa (4 June and 25 June 2010), and both indicate a discrepancy in wind direction for patches of light UWI winds.

Average bias levels and standard deviations of UWI winds relative to FG winds are displayed in Table 1. From this it follows that the bias of UWI winds was somewhat more negative (-1.08 m/s, was -1.03 m/s), being around -0.2 m/s more negative than for nominal data in 2000.

On a longer time scale seasonal bias trends are observed (see Figure 1). As was highlighted in previous cyclic reports, it is believed that the yearly trend is partly induced by changing local geophysical conditions.

The standard deviation of UWI wind speed versus ECMWF FG has, compared to Cycle 157, was reduced (1.33 m/s, was 1.38 m/s).

For Cycle 158 the (UWI - FG) direction standard deviations were mostly ranging between 20 and 40 degrees (Figure 8). An increased scatter and volatility is observed near the end of Cycle 158. Average STDV for UWI wind direction was worse than for Cycle 157 (28.7 degrees, was 24.9 degrees). For at ECMWF de-aliased winds (Figure 10) performance is stable (STDV 18.4, was 18.3 degrees).

	Cycle 157		Cycle 158	
	UWI	CMOD4	UWI	CMOD4
speed STDV	1.38	1.38	1.33	1.34
node 1-2	1.40	1.38	1.40	1.39
node 3-4	1.32	1.31	1.33	1.32
node 5-7	1.31	1.31	1.28	1.28
node 8-10	1.33	1.33	1.28	1.28
node 11-14	1.39	1.39	1.30	1.31
node 15-19	1.37	1.38	1.32	1.34
speed BIAS	-1.03	-1.03	-1.08	-1.09
node 1-2	-1.59	-1.57	-1.56	-1.55
node 3-4	-1.34	-1.30	-1.34	-1.31
node 5-7	-1.07	-1.05	-1.11	-1.10
node 8-10	-0.88	-0.89	-0.94	-0.95
node 11-14	-0.82	-0.84	-0.89	-0.92
node 15-19	-0.83	-0.87	-0.91	-0.95
direction STDV	24.9	18.3	28.7	18.4
direction BIAS	-2.1	-2.3	-2.1	-2.4

Table 1: Biases and standard deviation of ERS-2 versus ECMWF FG winds in m/s for speed and degrees for direction.

2.5   Scatterplots

Scatterplots of FG winds versus ERS-2 winds are displayed in Figures 13 to 16. Values of standard deviations and biases are slightly different from those displayed in Table 1. Reason for this is that, for plotting purposes, the in 0.5 m/s resolution ERS-2 winds have been slightly perturbed (increases scatter with 0.02 m/s), and that zero wind-speed ERS-2 winds have been excluded (decreases scatter by about 0.05 m/s).

The scatterplot of UWI wind speed versus FG (Figure 13) is very similar to that for (at ECMWF inverted) de-aliased CMOD4 winds (Figure 15). It confirms that the ESACA inversion scheme is working properly.

Winds derived on the basis of CMOD5 are displayed in Figure 16. The relative standard deviation is lower than for CMOD4 winds (1.33 m/s versus 1.37 m/s). Compared to ECMWF FG, CMOD5 winds are 0.65 m/s slower.

Figure Captions

Figure 1: Evolution of the performance of the ERS-2 scatterometer averaged over 5-weekly Cycles from 12 December 2001 (Cycle 69) to 5 July 2010 (end Cycle 158) for the UWI product (solid, star) and de-aliased winds based on CMOD4 (dashed, diamond). Results are based on data that passed the UWI QC flags. For Cycle 85 two values are plotted; the first value for a global set, the second one for a regional set (for details see

the corresponding cyclic report). Dotted lines represent values for Cycle 59 (5 December 2000 to 17 January 2001), i.e. the last stable Cycle of the nominal period. From top to bottom panel are shown the normalized distance to the cone (CMOD4 only) the standard deviation of the wind speed compared to FG winds, the corresponding bias (for UWI winds the extremes in node-wise averages are shown as well), and the standard deviation of wind direction compared to FG.

Figure 2: Average number of observations per 12H and per 125km grid box (top panel) and wind climate (lower panel) for UWI winds that passed the UWI flags QC and a check on the collocated ECMWF land and sea-ice mask.

Figure 3: The same as Figure 2, but now for the relative bias (top panel) and standard deviation (lower panel) with ECMWF first-guess winds.

Figure 4: Ratio of $< \sigma_0^{0.625} > / < \mathrm{CMOD4(FirstGuess)}^{0.625} >$ converted in dB for the fore beam (solid line), mid beam (dashed line) and aft beam (dotted line), as a function of incidence angle for descending and ascending tracks. The thin lines indicate the error bars on the estimated mean. First-guess winds are based on the in time closest (+3h, +6h, +9h, or +12h) T799 forecast field, and are bilinearly interpolated in space.

Figure 5: Time series of the difference in incidence angle between the fore and aft beam. Red stars indicate the occurrences for which the combined k_p-yaw flag was set.

Figure 6: Mean normalized distance to the cone computed every 6 hours for nodes 1-2, 3-4, 5-7, 8-10, 11-14 and 15-19). The dotted curve shows the number of incoming triplets in logarithmic scale (1 corresponds to 60,000 triplets) and the dashed one indicates the fraction of complete (based on the land and sea-ice mask at ECMWF) sea-located triplets rejected by ESA flags, or by the wind inversion algorithm (0: all data kept, 1: no data kept).

Figure 7: Mean (solid line) and standard deviation (dashed line) of the wind speed difference UWI - first guess for the data retained by the quality control.

Figure 8: Same as Fig. 7, but for the wind direction difference. Statistics are computed for winds stronger than 4 m/s.

Figures 9 and 10: Same as Fig. 7 and 8 respectively, but for the de-aliased CMOD4 data.

Figure 11: Locations of data during Cycle 158 for which UWI winds are more than 8 m/s weaker (top panel) respectively stronger (lower panel) than FG, and on which QC on UWI flags and the ECMWF land/sea-ice mask was applied.

Figure 12: Comparison of UWI winds (in red) with ECMWF FG winds (in blue) for a case on 6 June 2010 (top panel) and a case on 25 June 2010 (lower panel), both near the coast of West Africa.

Figure 13: Two-dimensional histogram of first guess and UWI wind speeds, for the data kept by the UWI flags, and QC based on the ECMWF land and sea-ice mask. Circles denote the mean values in the y-direction, and squares those in the x-direction.

Figure 14: Same as Fig. 13, but for wind direction. Only winds stronger than 4m/s are taken into account.

Figure 15: Same as Fig. 13, but for de-aliased CMOD4 winds.

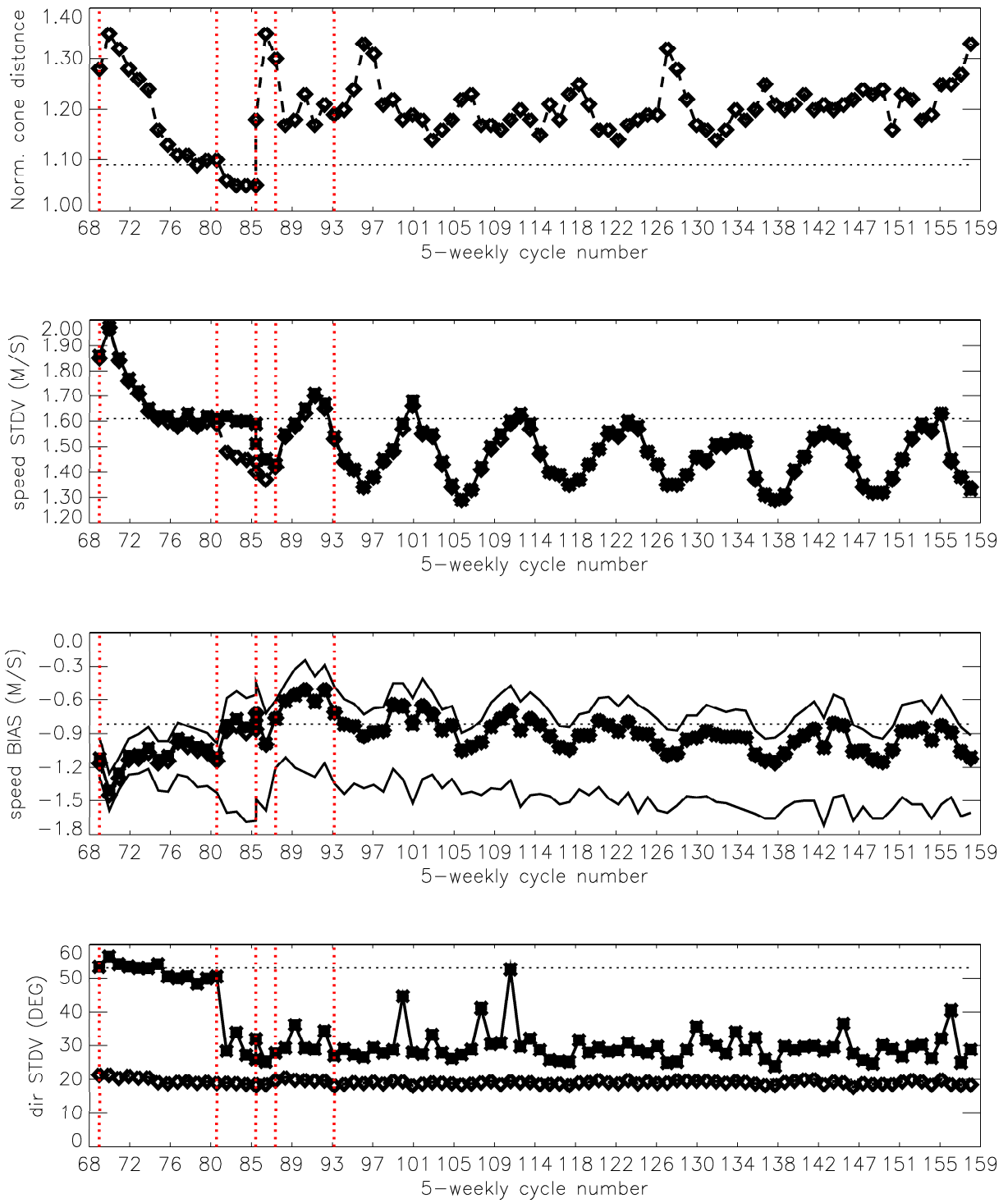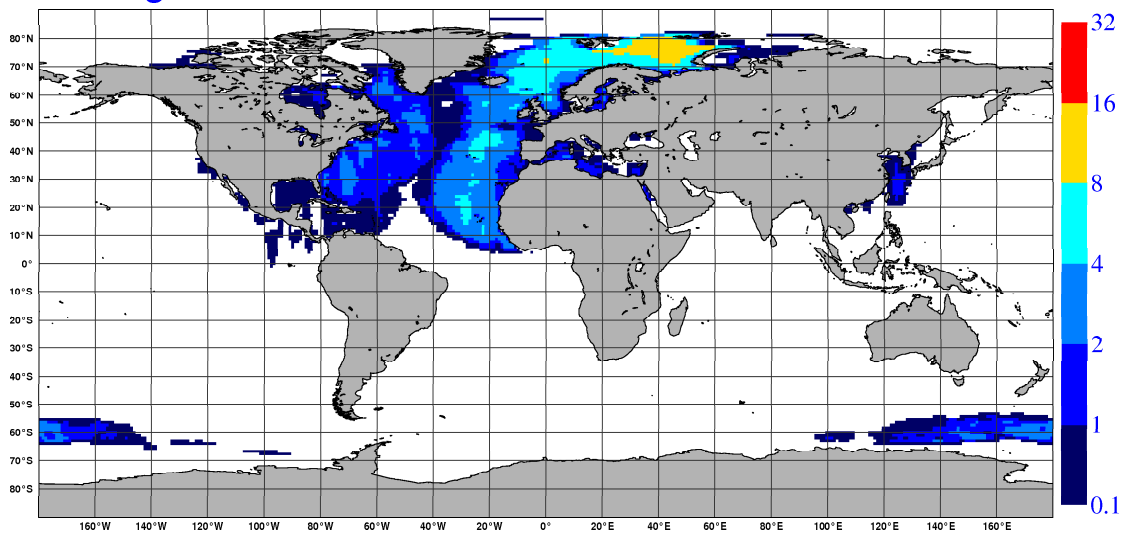**Figure 16:** Same as Fig. 13, but for de-aliased CMOD5 winds.

Figure 1

NOBS (ERS-2 UWI), per 12H, per 125km box
average from 2010060100 to 2010070518 GLOB:1.71

AVERAGE (ERS-2 UWI), in m/s.
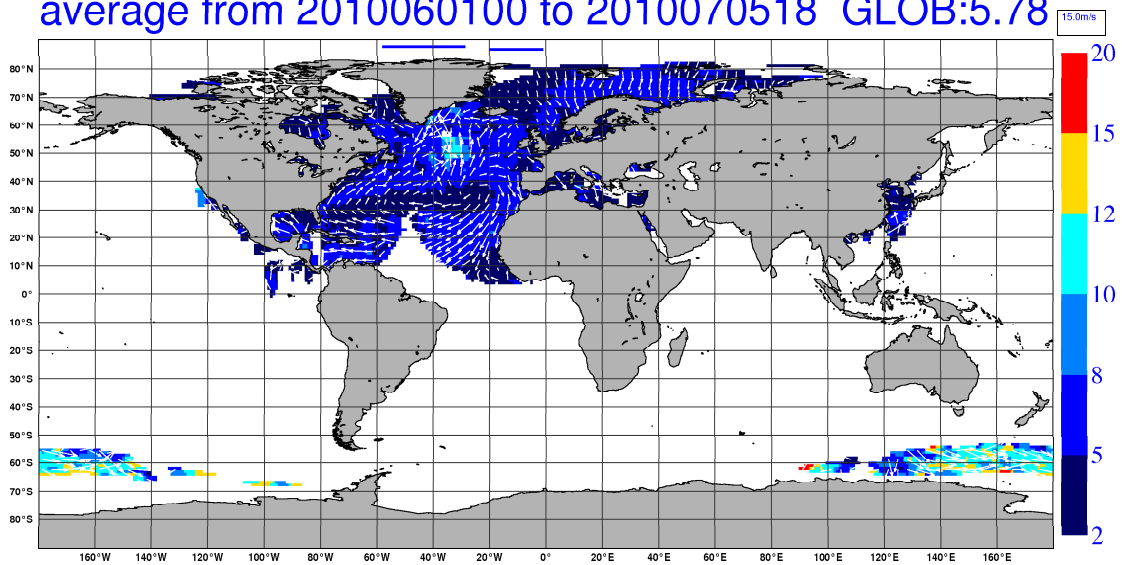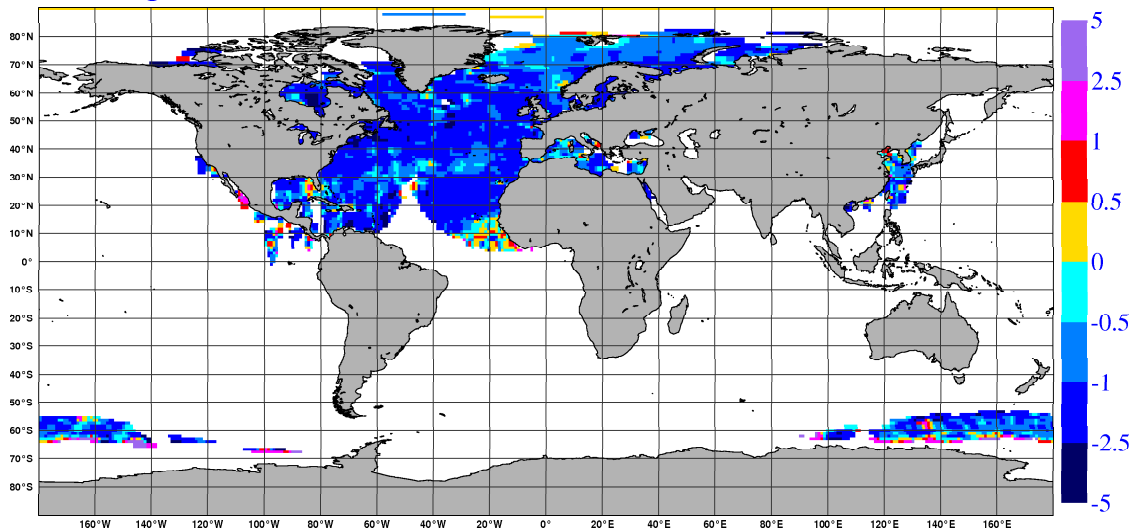average from 2010060100 to 2010070518 GLOB:5.78

Figure 2

BIAS (ERS-2 UWI vs FIRST-GUESS), in m/s.
average from 2010060100 to 2010070518 GLOB:-1.09

STDV (ERS-2 UWI vs FIRST-GUESS), in m/s.
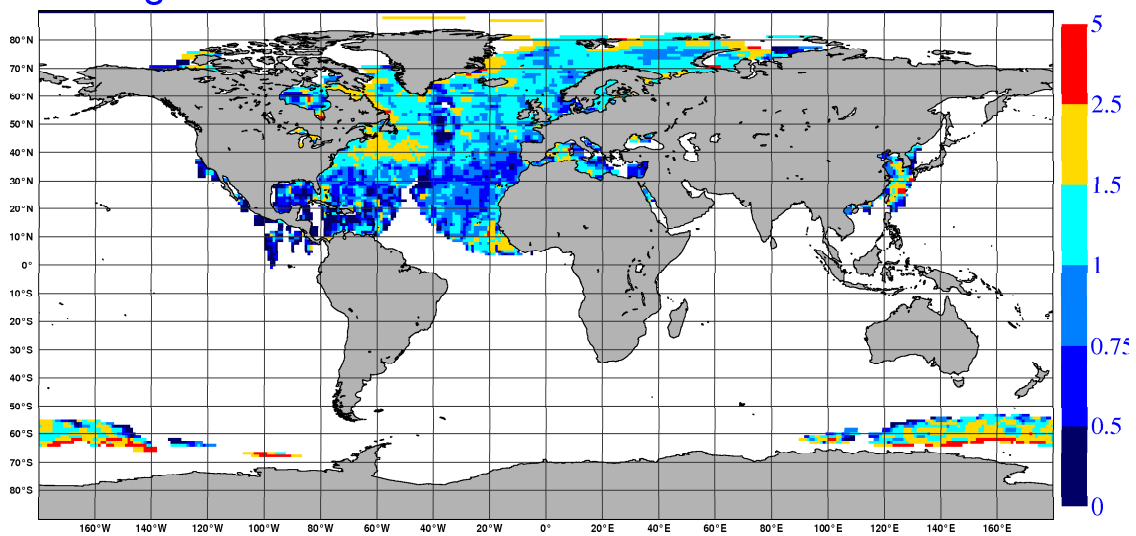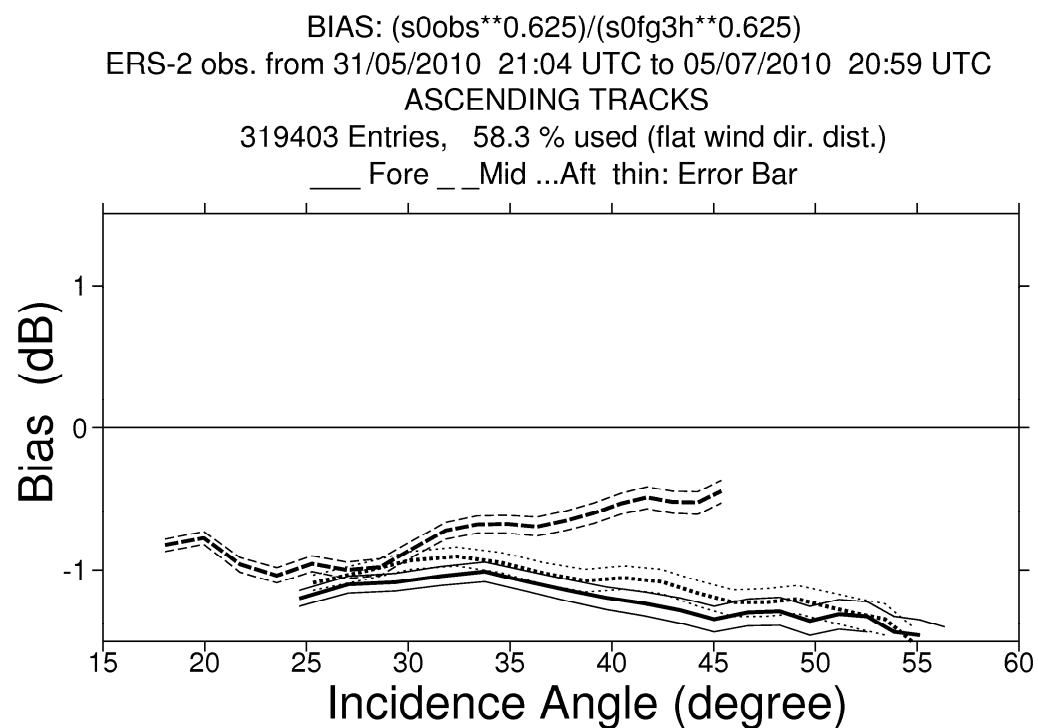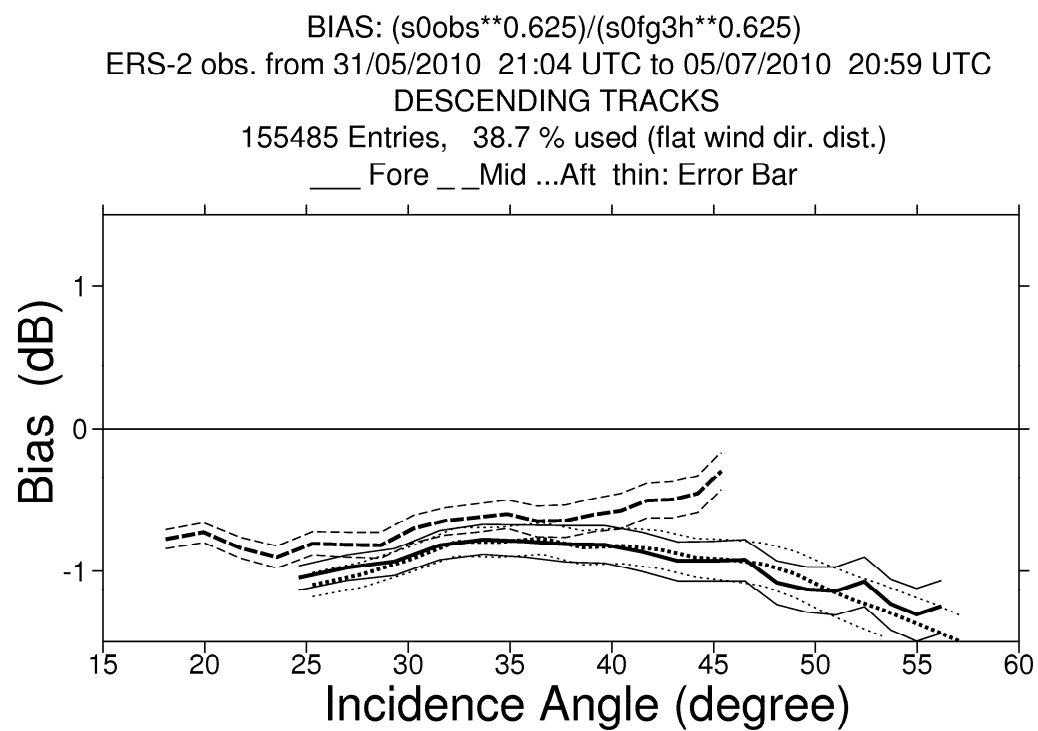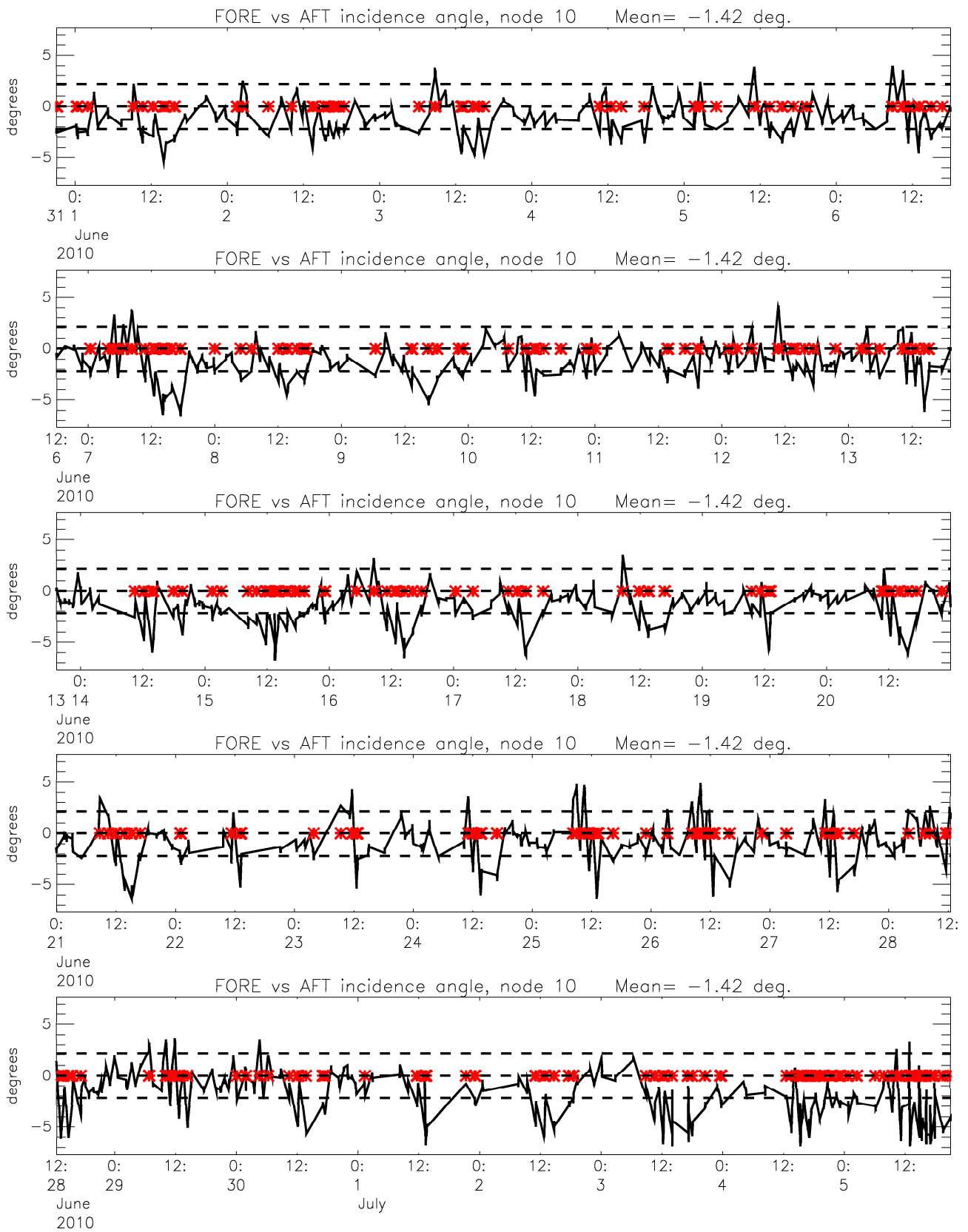average from 2010060100 to 2010070518 GLOB:1.08

Figure 3

BIAS: (s0obs**0.625)/(s0fg3h**0.625)
ERS-2 obs. from 31/05/2010 21:04 UTC to 05/07/2010 20:59 UTC
DESCENDING TRACKS
155485 Entries,   38.7 % used (flat wind dir. dist.)
____ Fore _ _Mid ...Aft thin: Error Bar

BIAS: (s0obs**0.625)/(s0fg3h**0.625)
ERS-2 obs. from 31/05/2010 21:04 UTC to 05/07/2010 20:59 UTC
ASCENDING TRACKS
319403 Entries,   58.3 % used (flat wind dir. dist.)
____ Fore _ _Mid ...Aft thin: Error Bar

Figure 4

Figure 5

Monitoring of Sigma0 triplets versus CMOD4 for ERS-2

from 2010060100 to 2010070518

(solid) mean normalised distance to the cone over 6 h

(dashed) fraction of complete sea-point observations rejected by ESA flag or CMOD4 inversion

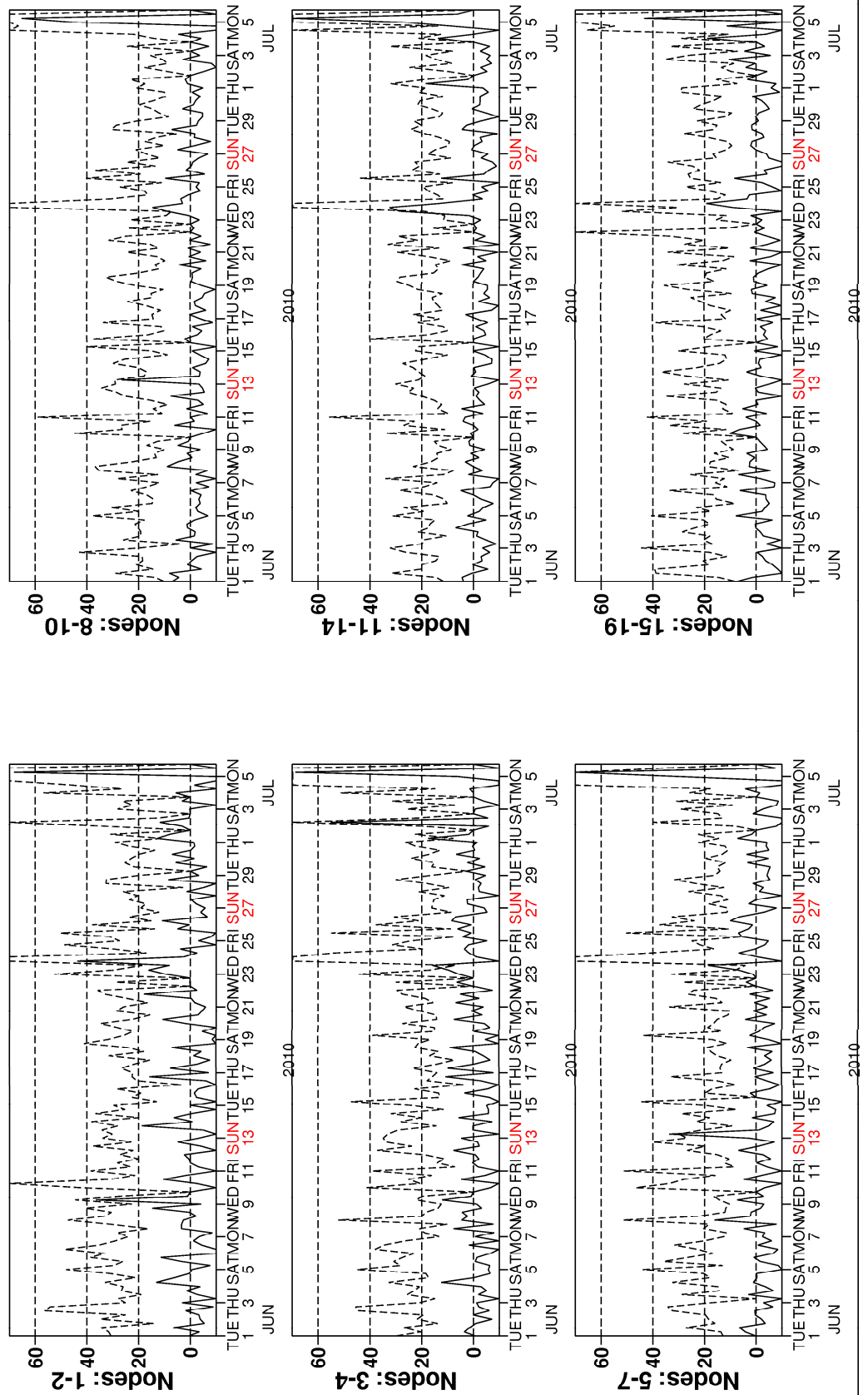(dotted) total number of data in log. scale (1 for 60000)

Figure 6

Figure 7

12
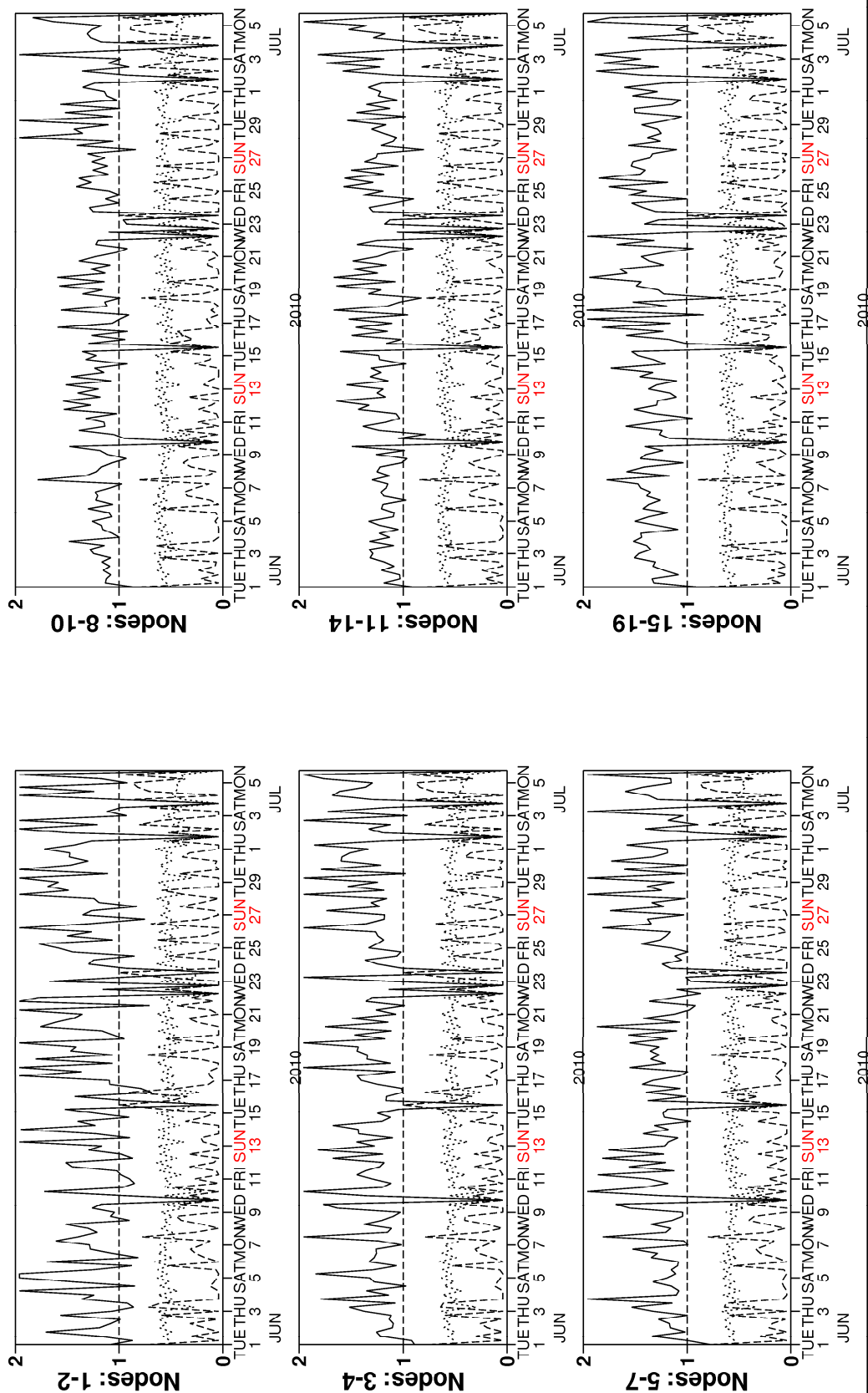
Monitoring of UWI winds versus First Guess for ERS-2

from 2010060100 to 2010070518

(solid) wind direction bias UWI - First Guess over 6h (deg.)

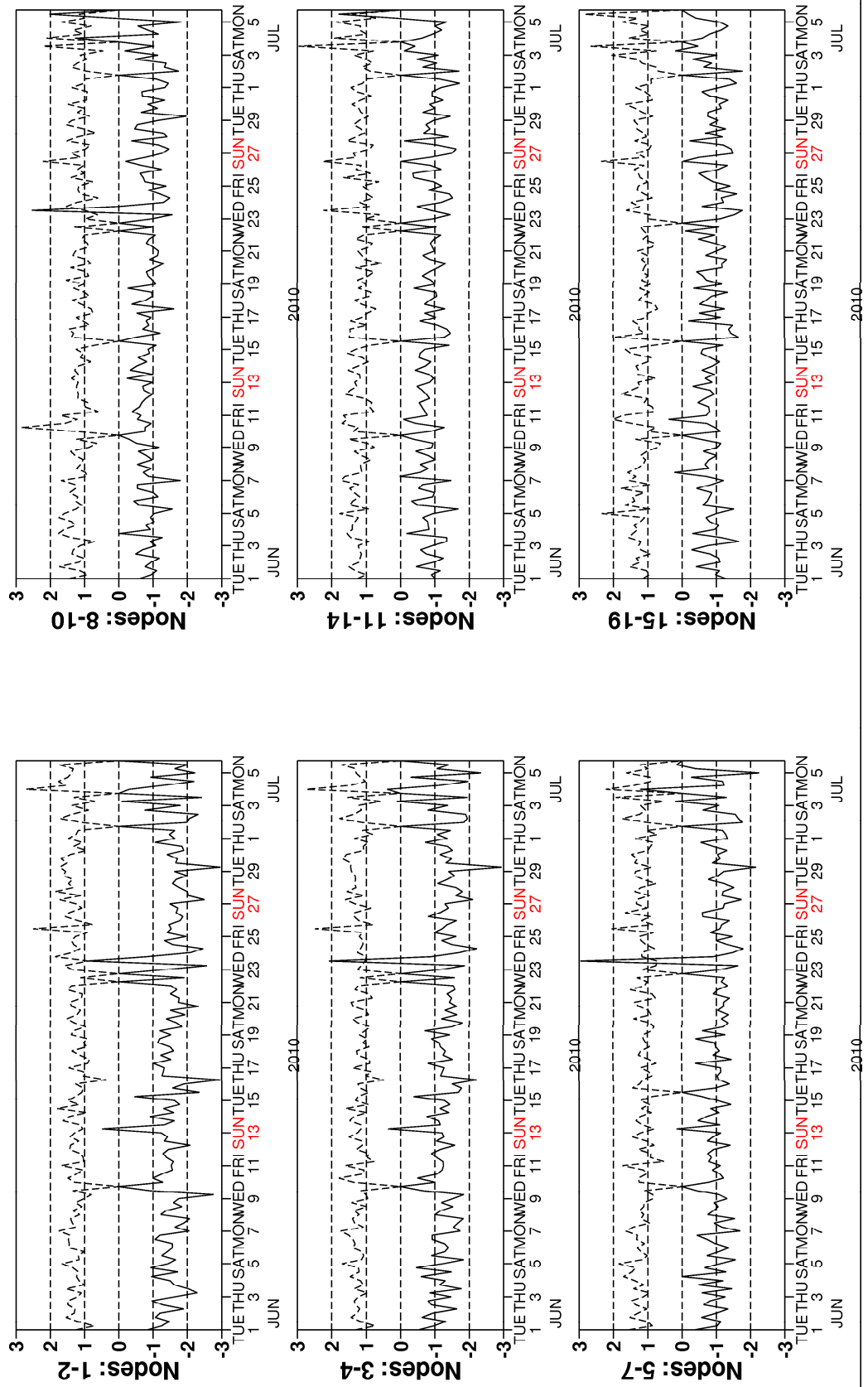(dashed) wind direction standard deviation UWI - First Guess over 6h (deg.)

Figure 8

13

Monitoring of de-aliased CMOD4 winds versus First Guess for ERS-2

from 2010060100 to 2010070518

(solid) wind speed bias CMOD4 - First Guess over 6h (deg.)

(dashed) wind speed standard deviation CMOD4 - First Guess over 6h (deg.)

Figure 9

Monitoring of de-aliased CMOD4 winds versus First Guess for ERS-2

from 2010060100 to 2010070518

(solid) wind direction bias CMOD4 - First Guess over 6h (deg.)

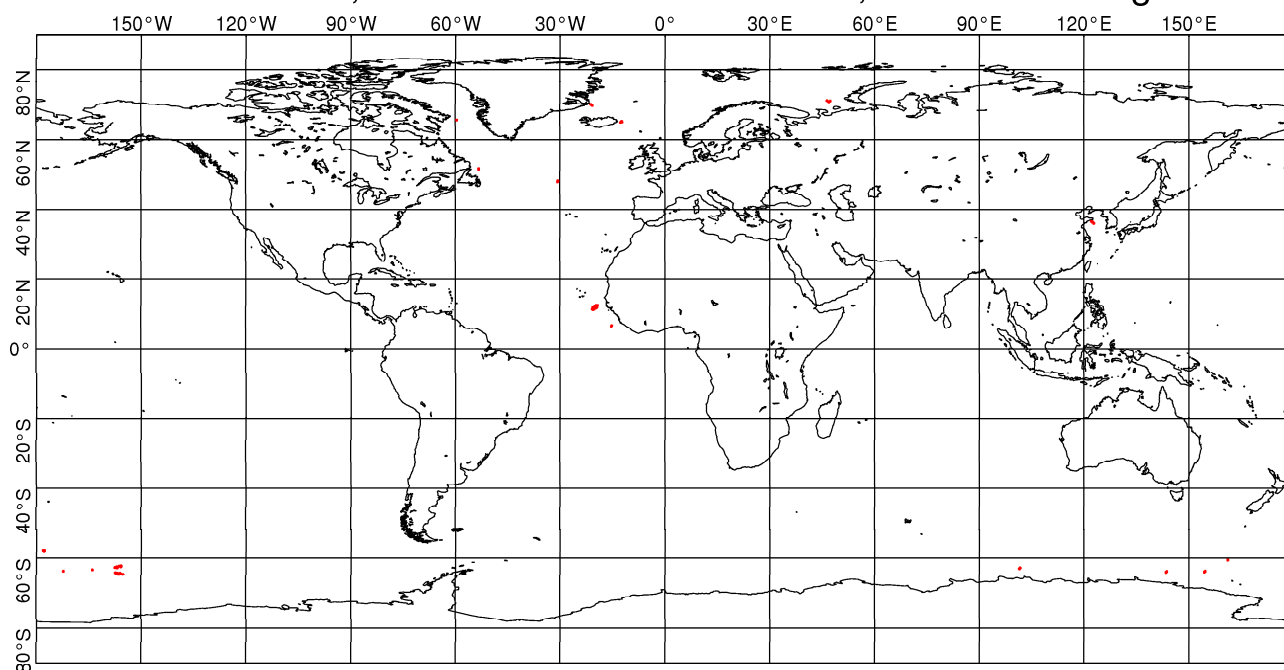(dashed) wind direction standard deviation CMOD4 - First Guess over 6h (deg.)

Figure 10

15
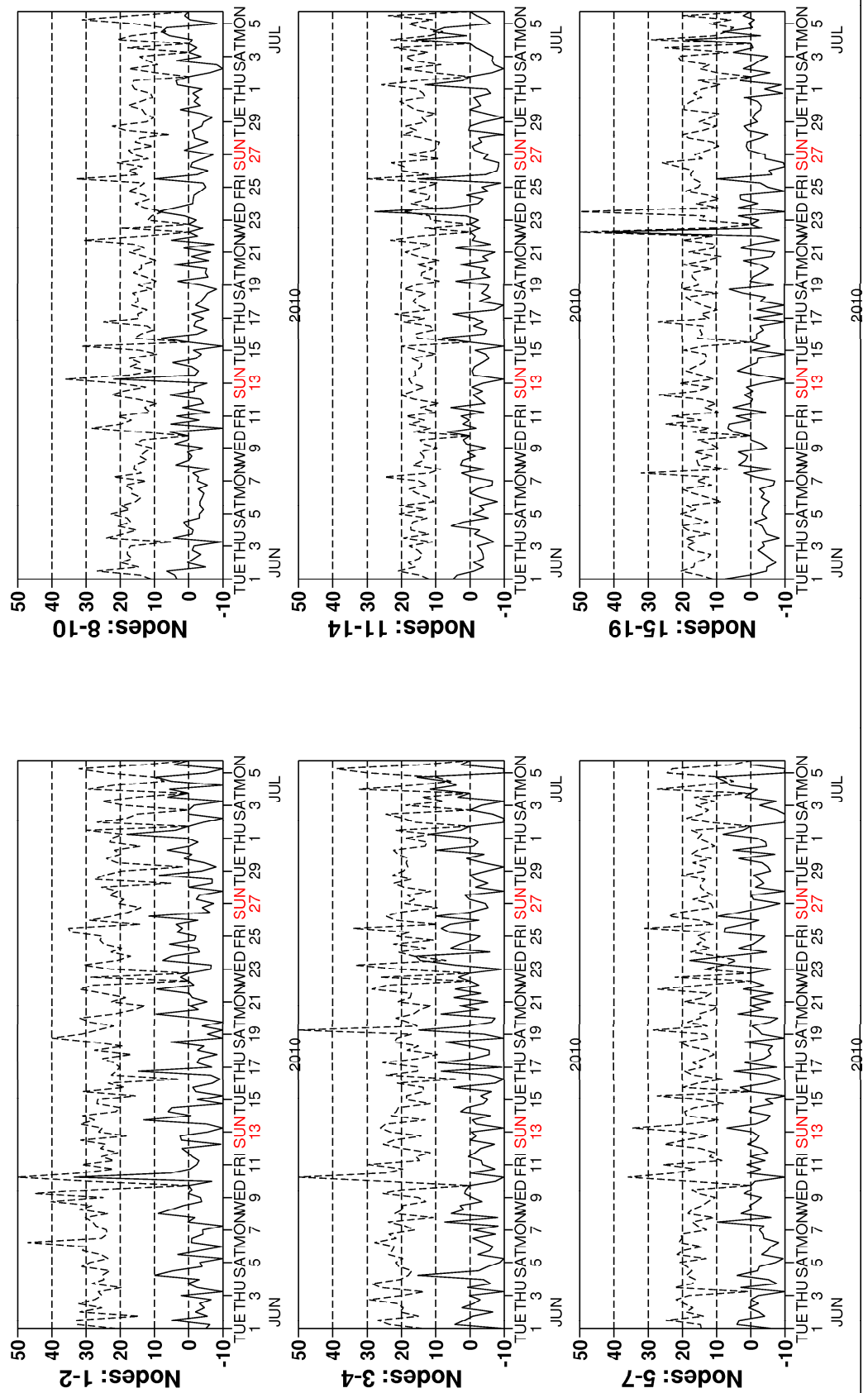
UWI winds more than 8 m/s weaker than ECMWF First Guess
CYCLE 158, 2010060100 to 2010070518, QC on ESA flags

UWI winds more than 8 m/s stronger than ECMWF First Guess
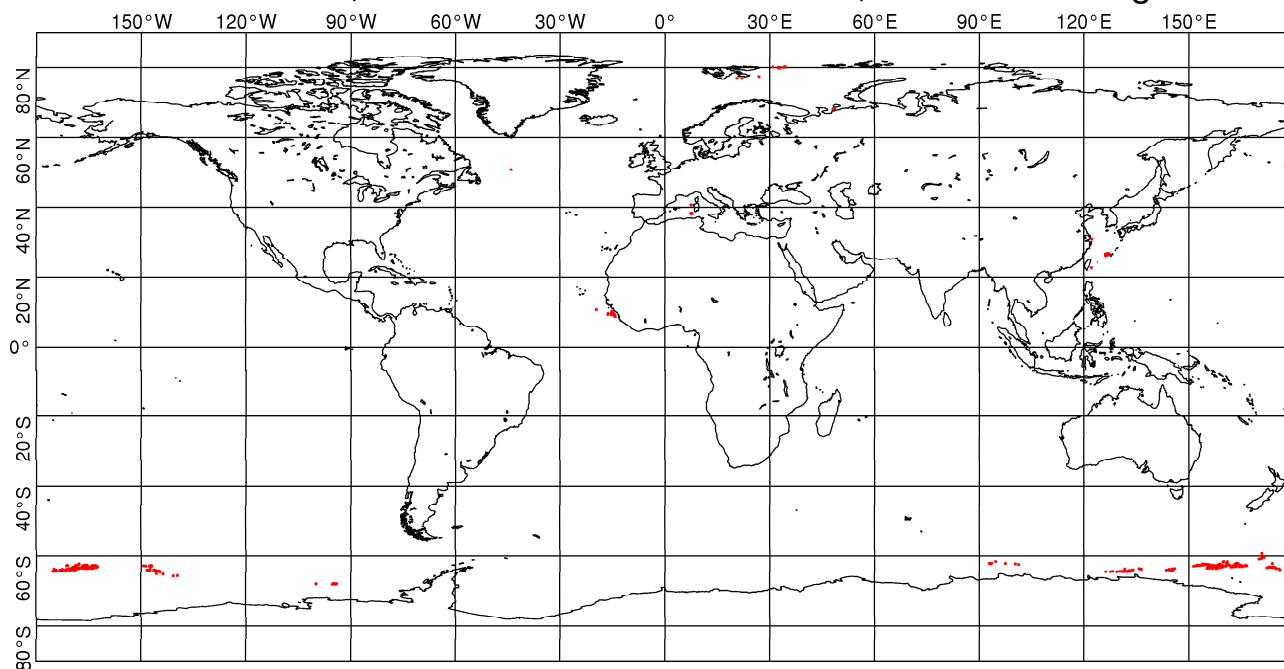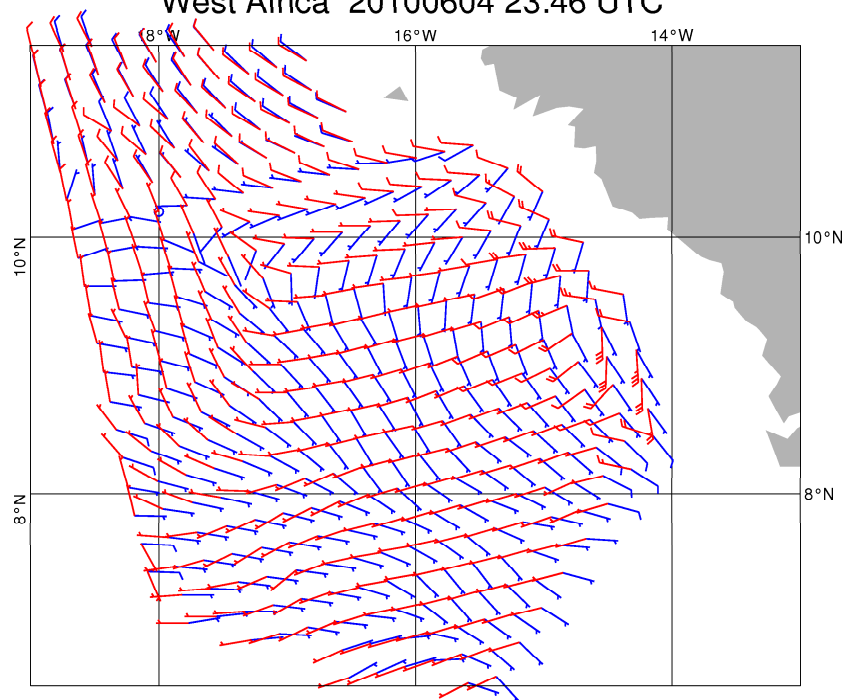### CYCLE 158, 2010060100 to 2010070518, QC on ESA flags

Figure 11

UWI winds (red) versus ECMWF FG winds (blue)
West Africa 20100604 23:46 UTC

UWI winds (red) versus ECMWF FG winds (blue)
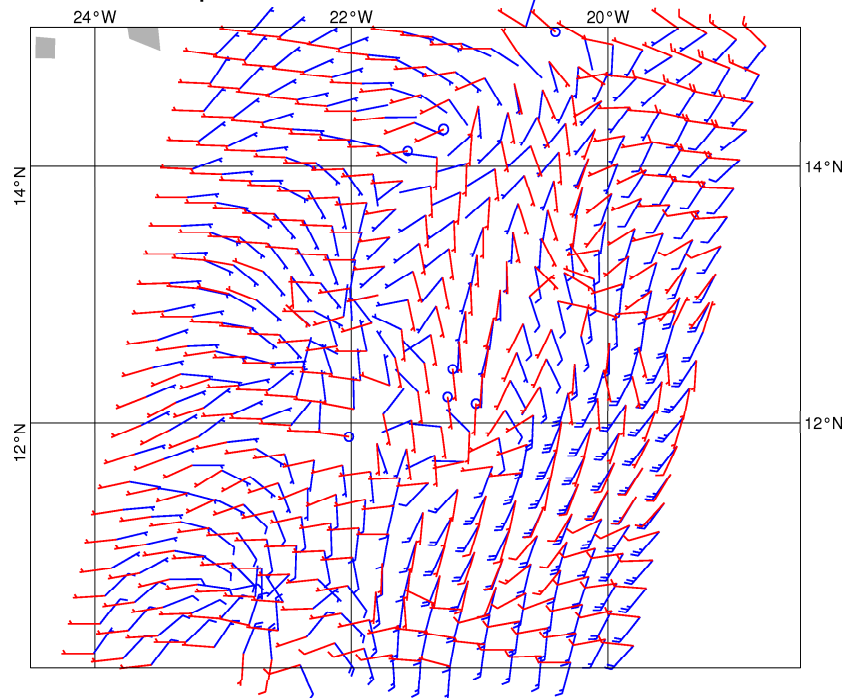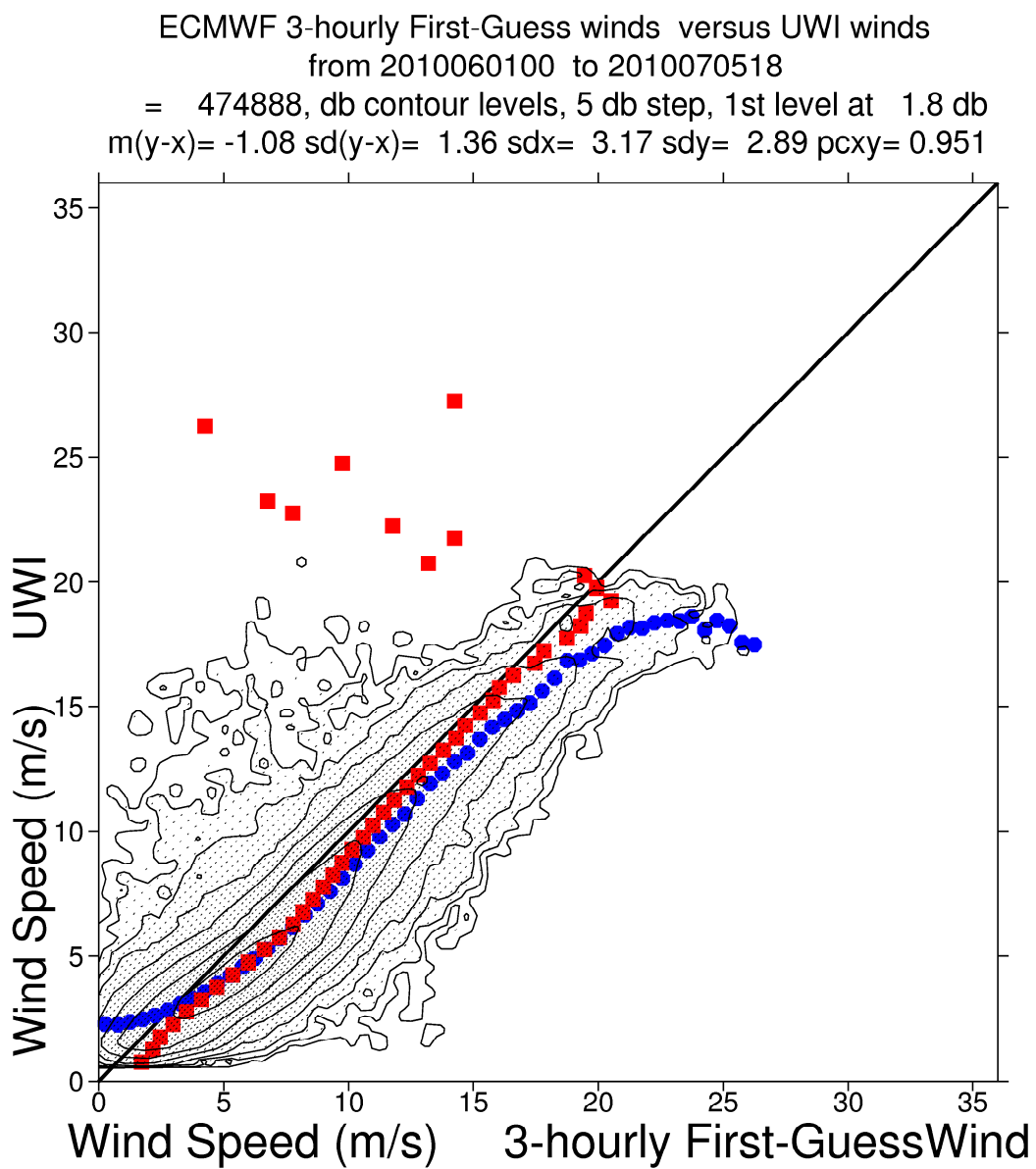Cape Verde 20100625 11:46 UTC

Figure 12

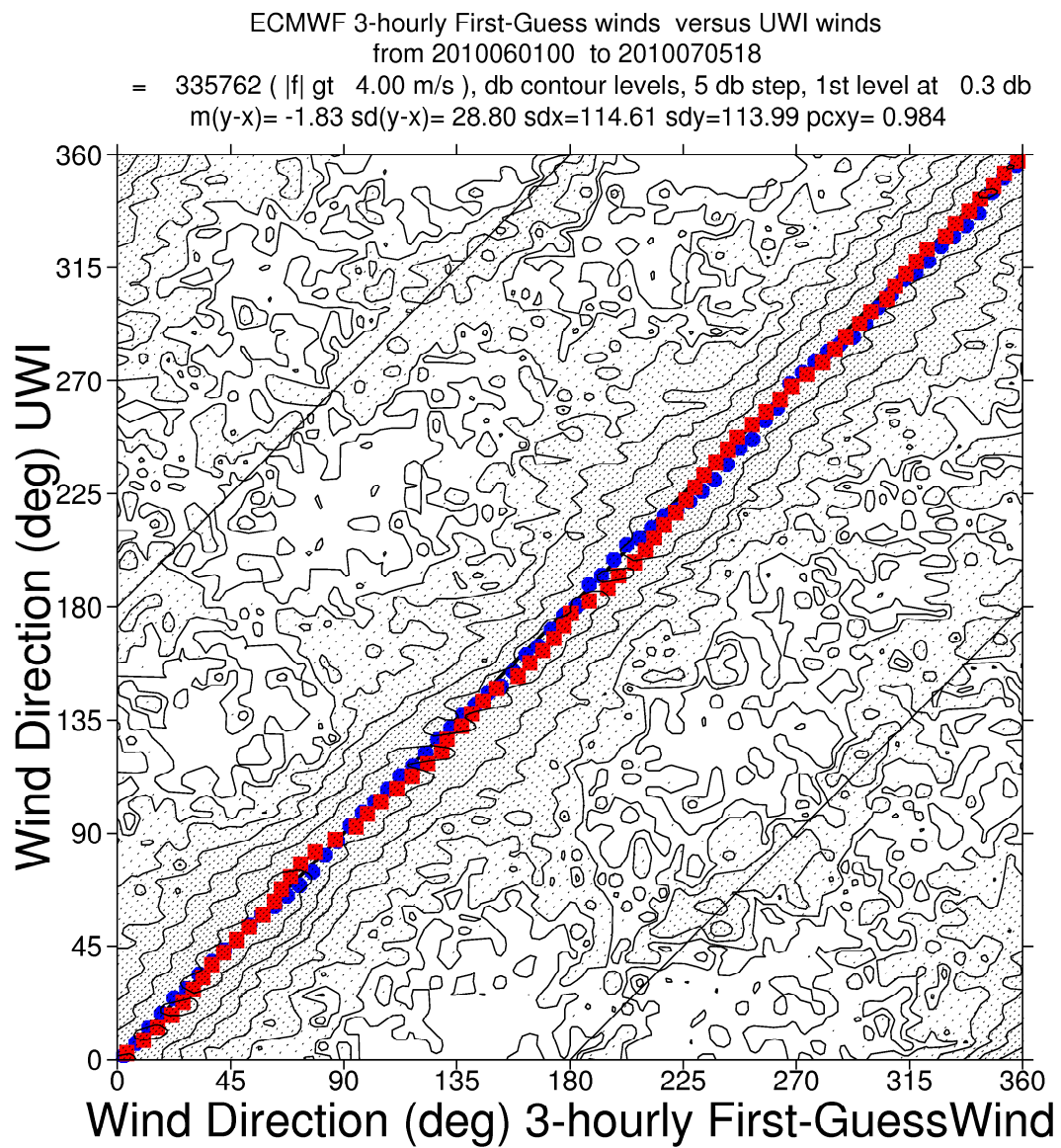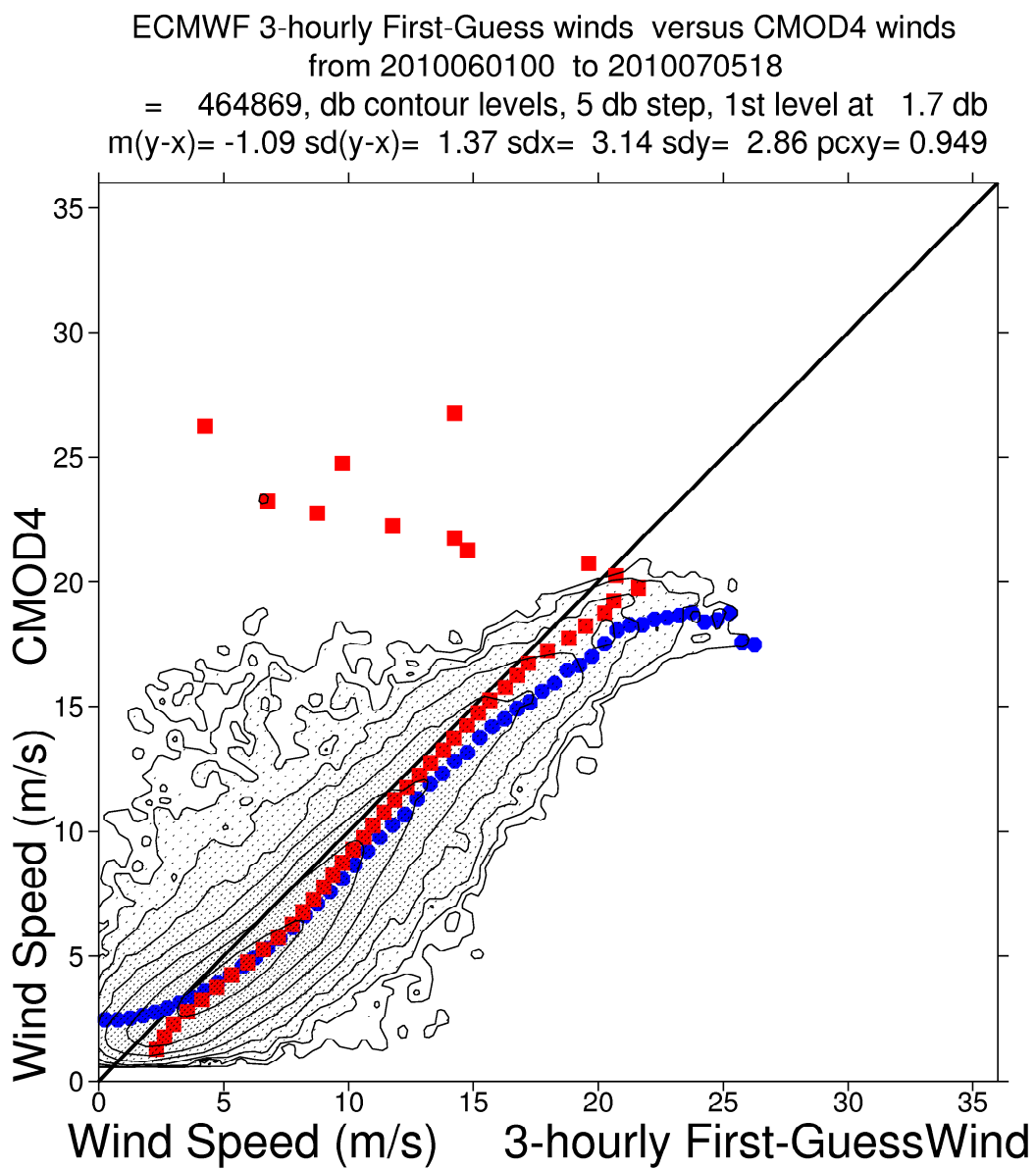ECMWF 3-hourly First-Guess winds versus UWI winds
from 2010060100 to 2010070518
=   474888, db contour levels, 5 db step, 1st level at   1.8 db
m(y-x)= -1.08 sd(y-x)= 1.36 sdx= 3.17 sdy= 2.89 pcxy= 0.951

Figure 13

ECMWF 3-hourly First-Guess winds versus UWI winds
from 2010060100 to 2010070518
=   335762 (|f| gt   4.00 m/s), db contour levels, 5 db step, 1st level at   0.3 db
m(y-x)= -1.83 sd(y-x)= 28.80 sdx=114.61 sdy=113.99 pcxy= 0.984

Figure 14

Figure 15

ECMWF 3-hourly First-Guess winds versus CMOD5 winds
from 2010060100 to 2010070518
= 450087, db contour levels, 5 db step, 1st level at 1.5 db
m(y-x)= -0.65 sd(y-x)= 1.33 sdx= 3.08 sdy= 3.02 pcxy= 0.951

Figure 16